CHEMISTRY OF MATERIALS

Communication

pubs.acs.org/cm

Elucidating the Solvation Structure and Dynamics of Lithium Polysulfides Resulting from Competitive Salt and Solvent Interactions

Nav Nidhi Rajput,[*,†,⊥] Vijayakumar Murugesan,[‡,⊥] Yongwoo Shin,[†] Kee Sung Han,[‡,⊥] Kah Chun Lau,[§,∥] Junzheng Chen,[‡] Jun Liu,[‡,⊥] Larry A. Curtiss,[§,⊥] Karl T. Mueller,[‡,⊥] and Kristin A. Persson[*,†,⊥]

[†]Lawrence Berkeley National Laboratory, Berkeley, California 94720, United States

[‡]Pacific Northwest National Laboratory, Richland, Washington 99352, United States

[§]Materials Science Division, Argonne National Laboratory, Argonne, Illinois 60439, United States

[∥]Department of Physics and Astronomy, California State University, Northridge, California 91330, United States

[⊥]Joint Center for Energy Storage Research (JCESR), Lemont, Illinois 60439, United States

Supporting Information

Designing optimal electrolytes is key to enhancing the performance of energy storage devices,especially relating to cycle life, efficiency, and stability.[1] Specifically, for future beyond-Li ion energy storage, there is still ample room for electrolyte improvements. Among the candidates for higher gravimetric energy storage, the Li−S battery is considered quite promising, owing to its theoretical specific energy density (2600 Wh/kg) and specific capacity (1675 mAh/g) and significantly lower cost as compared to state-of-art lithium-ion batteries.[2−4] However, despite these attractive attributes, successful commercialization of Li−S batteries is currently hindered by poor cycling performance and capacity retention that is primarily caused by the parasitic reactions between the Li metal anode and dissolved polysulfide (PS) species from the cathode during the cycling process.[3,5] Most of the efforts to overcome this degradation mechanism has focused on suppressing the dissolution of PS species and/or protecting the negative electrode using confinement strategies or protective layers. However, these additional components not only fail to block completely the PS species but also restrict the volumetric energy density.[2,6] In contrast, less attention has been given to designing optimal electrolytes with reduced PS solubility and improved electrochemical stability. Traditional Li salts used in Li-ion batteries (eg., $LiPF_6$, $LiBF_4$, LiBOB, $LiBF_2C_2O_4$) and solvents (eg., ester, carbonates, phosphates) are unsuitable for Li−S battery applications due to their parasitic reactions with PSs.[2] Hence, rational selection or design of the electrolyte is critical in controlling the deleterious shuttle reactions and protecting the electrode surface. So far, 1 M lithium bis(trifluoromethanesulfonyl)imide (Li-TFSI) in a binary solvent mixture of 1,3-dioxolane and 1,2-dimethoxyethane (DOL:DME) is considered as one of the most suitable electrolytes for Li−S cells.[2,5] However, despite its wide usage, the DOL:DME solvent system provides significant PS solubility, which enables the shuttle process and subsequent parasitic reactions.[2] Therefore, to develop electrolytes with low solubility, high chemical stability, and low viscosity, it is important to improve our understanding of the solvation structure and dynamics of the intermediate PS species formed during discharge. Ion solvation in electrolytes is composed of highly correlated ion−ion and ion−solvent interactions spanning wide spatial and temporal ranges. Currently, there is limited understanding of the solvation structure of various types of PS species (Li_2S_x; x = 1 to 8) formed during the discharge process. Experimental efforts based on spectroscopic techniques have mostly focused on specific constituents of the electrolyte and do not comprehensively report the solvation structure of PS species.[7,8] Ab initio based computational methods have provided valuable insights about the disproportionation and intermolecular association of PSs in Li−S electrolyte systems.[9−12] Nevertheless, comprehensive understanding regarding the evolution of solvation phenomena with respect to the PS chain length and solvent system remains elusive. Classical molecular dynamics (MD) simulations are well suited to obtain the needed molecular level understanding of nonreactive interactions and dynamics of multicomponent systems covering larger temporal and lateral scales. As per our knowledge, there is no previous work on understanding bulk structural and dynamical properties of PSs using classical molecular dynamics (MD) simulations mainly due to lack of effective force field parameters.

Various reaction mechanisms have been proposed during the discharge cycle using DFT calculations,[7,13] and spectroelectrochemical techniques,[7,14] reporting a variety of possible PS reaction intermediates (S_8^{2-}, S_7^{2-}, S_6^{2-}, S_5^{2-}, S_4^{2-}, S_3^{2-}, S_2^{2-}). Although these different PS species are postulated to coexist in the solution through chemical equilibrium,[2] it is nevertheless likely that their interactions with the salt and solvent are to a first-order approximation independent of each other. Hence, in this work we focus on understanding the properties of individual PS species S_x; x = 2 to 8, cognizant of the fact that they may all be present in the solution at some state-of-charge (SOC). As the first step in this direction, we study the solvation structure and diffusion coefficient of 0.25 M Li_2S_x (x

Received: January 6, 2017
Revised: March 29, 2017
Published: March 31, 2017

DOI: 10.1021/acs.chemmater.7b00068
Chem. Mater. 2017, 29, 3375−3379

= 2 to 8) in DOL:DME (1:1) and 0.25 M Li_2S_x (x = 2 to 8) with 1 M Li(TFSI) dissolved in a DOL:DME solvent mixture using newly developed and well-benchmarked force field parameters. Details of the simulation procedure, force field, and experimental procedure are provided in the Supporting Information (SI). Note that although previous studies have reported the formation of sulfur radical anions during discharge, in this work, we focus on the dianions.[7]

The present work focuses on three key scientific studies pertaining to Li−S electrolytes: (1) how Li-PS intermediates interact with the solvent molecules and the Li-salt; (2) the effect of salt addition on solvation structure and dynamics; and (3) the effect of PS chain length on the structure and dynamics. We begin our analysis by elucidating the local environment of Li_2S_x in DOL:DME and Li_2S_x in Li(TFSI)/DOL:DME using radial distribution functions (RDF) and coordination numbers (CN) of Li^+−Li^+, Li^+−S_x^{2-}, Li^+−$TFSI^-$, Li^+−DOL, and Li^+−DME. Previous studies have reported that the terminal S atom plays an important role in the PS interactions with Li^+.[7,15] Hence, the terminal and inner S atom interactions within the Li^+−S_x^{2-} RDF for all PSs (except for Li_2S_2) are clearly distinguished (Figure S2). Figure 1a shows the RDF of Li_2S_2 in

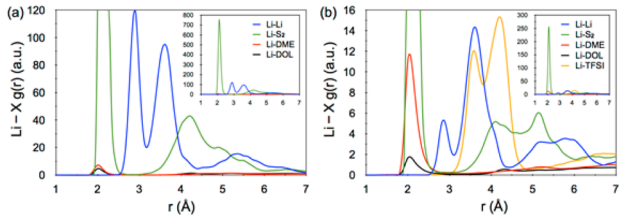

Figure 1. (a) Radial distribution function of Li^+−Li^+, Li^+−S_2^{2-}, Li^+−DME, Li^+−DOL in Li_2S_2/DOL:DME. (b) Radial distribution function of Li^+−Li^+, Li^+−S_2^{2-}, Li^+−DME, Li^+−DOL and Li^+−$TFSI^-$ in (Li_2S_2+LiTFSI)/DOL:DME.

an equimolar solvent mixture of DOL:DME. We observed very strong Li^+−S_2^{2-} interactions as indicated by a Li^+−S_2^{2-} RDF first peak at 2.1 Å followed by a shoulder at 4.2 Å. In contrast, the Li−solvent interaction is quite weak due to (1) the low dielectric constants of both DOL (ε = 7.0) and DME (ε = 7.2) and (2) the strong interaction between Li^+ and S_2^{2-}. The RDF signifying the Li^+−Li^+ correlation exhibits two sharp peaks followed by a shoulder at ∼5.4 Å illustrating highly ordered long-range (>5 Å) structures where the PSs acts as a bridge between the Li^+ ions through Li^+···S···Li^+ ionic chains. The snapshot in Figure S3a shows that Li_2S_2 is not well solvated and preferentially forms aggregates in the solution. Such agglomeration of Li_2S_2 is likely to result in an extremely low solubility of Li_2S_2 in DOL:DME. Previous experimental studies[16] have also reported weak Li−solvent interaction even in high donor number solvents such as DMSO (ε = 46.7) resulting in generally low solubility of Li_2S_2.[16] Hence, strong Li^+−S_2^{2-} bonding is presumed the primary cause for low solubility of Li_2S_2. Furthermore, it is likely that Li salts play an important role in controlling the solubility of PS intermediates.[16] Hence, to understand how the interaction strength between the Li^+ and S_x^{2-} changes with the addition of Li salt, we computed the RDF of Li_2S_2 in a solution with Li(TFSI) in DOL:DME solvent (Figure 1b). In this solution, although strong Li^+−S_2^{2-} interactions are still observed, a significant change is observed in the solvation structure around Li^+. Instead of two sharp peaks in the Li^+−Li^+ RDF, we observe a much smaller peak at 2.9 Å followed by a sharp peak at 3.6 Å and a broader shoulder at 5.4 Å. Similarly, for the Li^+−S_2^{2-} RDF the electrolyte exhibits a single peak at 2.1 Å with low intensity and a much broader shoulder at larger distances. The Li^+−$TFSI^-$ RDF shows two peaks centered at 3.6 and 4.2 Å indicating a cis-conformation with bidentate and a trans-conformation with monodentate arrangements of the Li^+−$TFSI^-$ interactions, respectively.[17] The changes in the RDF of Li^+−Li^+ and Li^+−S_2^{2-} strongly indicates that $TFSI^-$ anions are competing for interaction with Li^+ and thereby weaken the Li^+−S_2^{2-} interactions leading to a disruption of the Li^+−S_2^{2-} cluster network. Decrease in the Li^+−Li^+ and Li^+−S_2^{2-} coordination numbers and an increase in Li^+−DME coordination number reveals the changes in the local environment around Li^+ with the addition of Li(TFSI) salt in Li_2S_2 (Figure S4). As the weakening of the Li^+−S_2^{2-} bond by $TFSI^-$ interactions allows more solvent molecules to coordinate with Li^+ we expect the solubility of Li_2S_2 to increase. We note that this effect is in contrast to common ion effect theory,[6] which predicts the solubility to decrease with the addition of salt. Furthermore, a closer look at the Li−solvent interactions reveals that the linearly structured ether DME has stronger interaction as compared to the cyclic ether DOL owing to higher oxygen donor denticity and structural flexibility.[18] Such preferential solvation of DME over DOL for Li^+ has also been reported by NMR experimental techniques. Despite the weakened Li^+−S_2^{2-} interaction and increased Li^+−solvent interactions due to the presence of $TFSI^-$, the enduring Li_2S_2 clustering network is likely to limit the solubility of the PS (Figure S3b).

Another, key parameter which affects the solubility is the PS chain length; hence we endeavor to understand how the coordination environment of Li^+ and S_x^{2-} changes as a function of PS chain length. Figure 2a and S5a presents the coordination between Li^+−Li^+ as a function of PS chain length in a neat solvent system (i.e., without Li(TFSI) salt). Well-defined sharp peaks at shorter distances (<5 Å) and broader peaks at longer distances (>5 Å) indicate an ordered polymeric structure present for lower polysulfide chains (i.e., S_x with $x \leq 4$). In fact, a well-defined peak at ∼7 Å (Figure S6a) suggests the formation of a long-range structured Li_2S_4 cluster with a size of ∼14 Å radius. This finding is in good agreement with the effective hydrodynamics radius determined by pulse field gradient NMR (see Figure S7).[5]

Recent DFT and AIMD results by Partovi-Azar et al.[8] also suggest the preferential tendency of Li_2S_4 toward forming large ionic clusters by analyzing cluster size up to $(Li_2S_4)_8$ due to computational limitation. As MD simulations are capable of studying larger length and time scales, we found the largest cluster formed is $(Li_2S_4)_{15}$ even at 0.25 M concentration (see Figure S8a). For higher order PSs (S_x^{2-} with x > 4), the Li^+−Li^+ RDF peaks shifts toward larger distances and for Li_2S_8 only a single main peak is observed at 4.1 Å, indicating the absence of long-ranged clustering (see Figure 2a). By analyzing the evolution in bonding of Li^+−S_x^{2-}, Li^+−DOL, and Li^+−DME for various PS species, it is clear that the Li^+−S_x^{2-} interaction weakens with an increase in PS chain length (see Figure S5). In particular, the Li^+ interaction with the inner S atoms changes and shifts toward larger distances (see Figure S2) showcasing the flexibility of higher order PSs in accommodating Li^+ in their first solvation shell. Nevertheless, the Li^+−solvent interaction (with preferential interaction with DME over DOL) is also increased at the cost of the Li^+−S_x^{2-} interaction strength. Such pronounced Li^+−solvent interaction correlates with the

DOI: 10.1021/acs.chemmater.7b00068
Chem. Mater. 2017, 29, 3375−3379

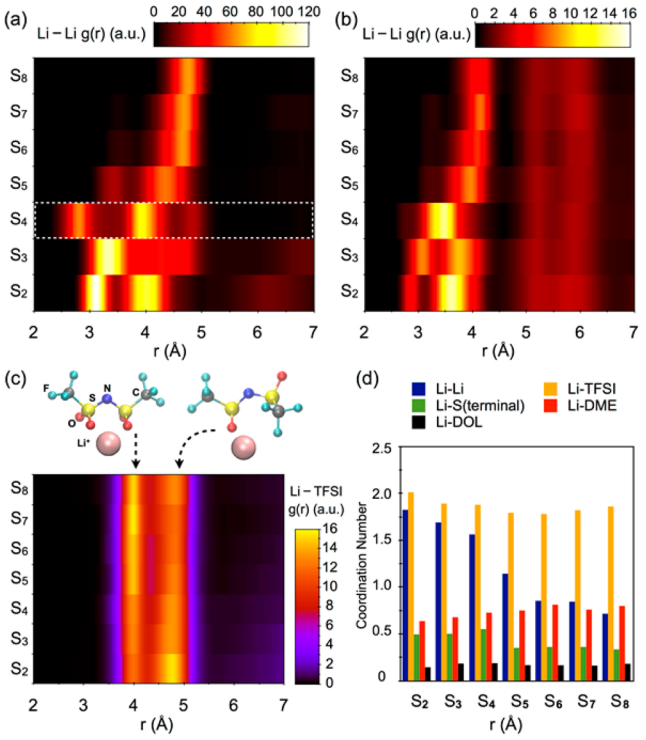

Figure 2. (a) Radial distribution function of Li^+–Li^+ in Li_2S_x (x = 2 to 8) in DOL:DME. (b) Radial distribution function of Li^+–Li^+ and (c) Li^+–$TFSI^-$ in Li_2S_x (x = 2 to 8) + Li(TFSI) in DOL:DME. (d) Coordination number of Li^+–Li^+, Li^+–$TFSI^-$, Li^+–S_x^{2-} (terminal), Li^+–DME, Li^+–DOL in Li_2S_x (x = 2 to 8) + Li(TFSI) in DOL:DME.

observed higher solubility of longer PS chains in a DOL:DME mixture.[16] Conversely, the extended (~few nm) polymeric structure formation can possibly lower the solubility of the shorter PS chains. This finding is in good agreement with our previous results that clustering (through polymerization) of lower order PSs lower their solubility.[11]

The effect of PS chain length on the local environment around Li^+ is observed for the case when a Li salt is added to the solution. Figures 2b and S5b show the RDF analyses of Li^+–Li^+ and Li^+–$TFSI^-$ for Li_2S_x (x = 2 to 8) in DOL:DME in the presence of the Li(TFSI) salt. The solvation structure of Li^+ as a function of PS species shows a similar trend as that observed in the neat solvent system discussed earlier. Multiple sharp peaks in Li^+–Li^+ RDF at shorter distances are observed for shorter PSs (S_x with $x \leq 4$), indicating clustering with extended-range PS structure. On the other hand, the absence of features at larger distances (>5 Å) in longer PSs represents the decrease in long-range structures such as aggregates and Li-rich domains. Hence, we can expect the solubility to increase with an increase in PS length even in the presence of the salt. The effect of the addition of Li salt is found to be minimal in smaller PSs; hence large clusters are still observed for (Li_2S_4 + LiTFSI)/DOL:DME solution (Figures S8b and S9). As one of the dominant PS species during the discharge process,[7,13] the large cluster observed for Li_2S_4 is likely to increase the electrolyte viscosity. This increase in viscosity, in turn, may contribute to the sharp voltage decline observed in the second region of the discharge profile, where liquid–liquid single phase reduction from dissolved Li_2S_8 to low order PSs is observed. As discussed earlier, the two peaks around 3.5 and 4.2 Å observed in the RDF of Li^+–$TFSI^-$ are assigned to bidentate and monodentate conformational arrangements, respectively (Figure 2c). With the increase in PS chain length, the probability of the bidentate conformation increases at the cost of the monodentate conformation. The bidentate conformation may weaken the Li^+–S_x^{2-} interaction in longer PS chains by two mechanisms (1) delithiation of PS anions that will enhance the solvent interaction with the Li^+ ions, and (2) increased oxygen coordination and steric hindrance from the $TFSI^-$ anions. Figure 2d shows the coordination number of Li^+–Li^+, Li^+–$TFSI^-$, Li^+–S_x^{2-}, Li^+–DOL, Li^+–DME interactions for the Li_2S_x (x = 2 to 8) + Li(TFSI) in DOL:DME solution. The terminal S atom is used to compute the coordination numbers of Li^+–S_x^{2-} and the RDF minima at ~5 Å, which defines the first coordination shell of the anion including both monodentate and bidentate orientations for Li^+–$TFSI^-$. The coordination number of Li^+–Li^+ in Li_2S_2 indicates that each Li^+ has 1.8 (~2) other Li^+ located within a radius of 4.4 Å, whereas Li_2S_8 has 0.76 (~1) other Li^+ ions located within 4.6 Å. It is observed that Li^+–Li^+ and Li^+–S_x^{2-} coordination numbers decrease with an increase in PS chain length indicating a significant change in Li^+ environment. Higher orders PSs are sufficient to provide the desired charge to Li^+ ions and the steric hindrance of PSs result in a lower coordination numbers for Li^+–S_x^{2-} and higher coordination numbers between Li^+ and the solvent. This in turn is expected to increase the solubility of larger PSs. In particular, the increase in coordination of Li^+ with DME is more significant as compared to Li^+ with DOL as a function of PS chain length due to the preferential coordination of DME with Li^+ over DOL as discussed earlier. We find that higher order PSs exist as monomers and show increased interaction with solvent molecules, which may result in faster reaction kinetics. In contrast, smaller PSs exist as dimers or clusters resulting in less interaction with the solvent molecules, which is likely to slow down the reaction kinetics. As a primary function of Li–S electrolytes is the efficient transport of ions between anode and cathode, while suppressing the dissolution of PS species, it is essential to understand the effect of solvation structure on the diffusion coefficient of ionic species, which in turns affects the conductivity. The translational dynamics is studied by extracting the self-diffusion coefficient of all ionic species using MD simulations as well as pulsed-field gradient (PFG) NMR (Figure 3).

Figure S10 shows the self-diffusion coefficients of Li^+, $TFSI^-$ and S_x^{2-} computed from MD simulations. It is observed that the diffusion coefficients of Li^+, $TFSI^-$ and S_x^{2-} decrease with increased PS chain length, which indicates sluggish dynamics of ionic species and possibly higher viscosity for solutions containing the larger PSs. Figure 3 shows a comparison between the self-diffusion coefficients obtained from MD simulations and PFG-NMR. The trends in self-diffusion coefficient are in good agreement; however, the simulation diffusion coefficients are consistently lower than the experimental counterparts owing to the well-known limitation of nonpolarizable force fields.[19] A significant decrease in diffusion coefficients for Li^+, $TFSI^-$, DOL as well as DME in Li(TFSI)/DOL:DME is observed as the concentration of Li(TFSI) increases for 0.25 to 3 M indicating that high viscosity and low ionic conductivity can be expected in highly concentrated electrolytes. For both Li_2S_x/DOL:DME and [Li_2S_x+Li(TFSI)]/DOL:DME the self-diffusion coefficient of the solutes as well as solvents decrease with an increase in PS chain length (Figure 3) again pointing to the high viscosity and low ionic conductivity of higher order PS solutions. As $TFSI^-$ is weakly coordinated to

DOI: 10.1021/acs.chemmater.7b00068
Chem. Mater. 2017, 29, 3375–3379

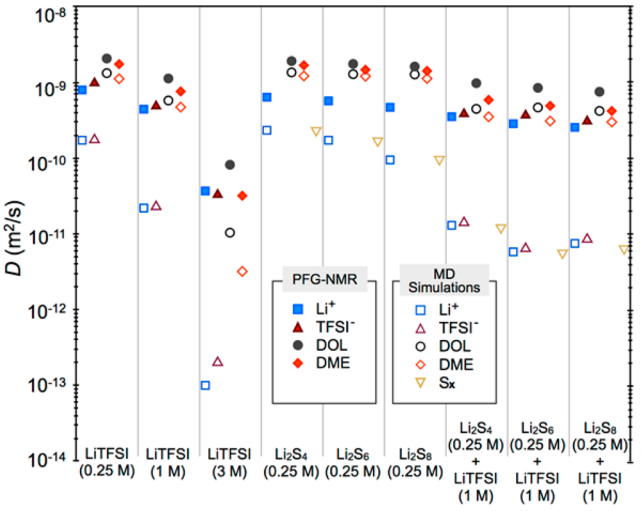

Figure 3. Self-diffusion coefficients of Li^+, $TFSI^-$, DOL, DME and PSs in 0.25 M, 1 and 3 M Li(TFSI), 0.25 M Li_2S_x (x = 4, 6, 8) in DOL:DME and 0.25 M Li_2S_x (x = 4, 6, 8) + 1 M Li(TFSI) in DOL:DME computed from MD simulations and PFG-NMR.

Li^+ compared to S_x^{2-}, its diffusion coefficient is higher than the diffusion coefficient of Li^+ and S_x^{2-} irrespective of the PS chain length. We note that in all systems considered in this work the self-diffusion coefficients follow the order $S_x^{2-} < Li^+ < TFSI^-$. Furthermore, both NMR and simulation results indicate that the self-diffusion coefficients of Li^+, PS anions and solvents are decreased by the addition of salt as well as an increase in PS chain length. Although enhanced ionic transport while maintaining low PS solubility is desirable for high performance Li−S battery operations, one of the most suitable electrolyte systems (Li(TFSI) in DOL:DME) exhibits both higher solubility of larger PS and slower dynamics for larger PS species. Thus, the recently proposed high concentration (lean) electrolytes[20] may in the case of Li(TFSI): DOL/DME consequently suffer from higher PS solubility and slower ionic diffusion of larger PSs. However, we also note that a more detailed understanding of the diffusion mechanism is required to understand if an increase in viscosity is fundamentally problematic in all Li−S electrolytes or if high transference numbers can balance out these effects.

Optimizing the lithium solvation environment in electrolyte solutions is key to controlling dissolution of polysulfide species. This work provides insights into the interactions between solute and solvent molecules in Li−S electrolytes and their dynamical properties as a function of polysulfide species and lithium salt present in the solution. Our results indicate large cluster formation in lower order polysulfides, whereas higher solubility is observed with an increase in polysulfide chain length. Stronger $Li^+-S_x^{2-}$ bonding is found to be the primary cause for the low solubility of lower order polysulfides. Furthermore, longer polysulfide chain lengths correlate with an increase in Li polysulfide−solvent interactions that allows for higher solubility, which may result in faster reaction kinetics. The addition of salt (Li−TFSI) weakens the strong $Li^+-S_x^{2-}$ networks due to competing interactions between $TFSI^-$ and polysulfide dianions with Li^+. This competition results in higher Li^+−solvent interactions and increased solubility, which is contrary to common ion effect theory. However, highly concentrated electrolytes might decrease the solubility of polysulfides. A high salt concentration also reduces the mobility of ionic species, which may negatively impact the ionic conductivity of the electrolyte. Overall, an improved understanding of the intramolecular interactions in the electrolyte will aid in designing solutions with limited solubility of detrimental species, without limiting functional properties such as ionic conductivity.

■ ASSOCIATED CONTENT

Supporting Information

The Supporting Information is available free of charge on the ACS Publications website at DOI: 10.1021/acs.chemmater.7b00068.

Details of computational and experimental methodology together with additional figures and tables (PDF)

■ AUTHOR INFORMATION

Corresponding Authors

*(N.N.R.) E-mail: nnrajput@lbl.gov. Tel.: +1-510-486-5389.
*(K.A.P.) E-mail: kapersson@lbl.gov. Tel.: +1-510-486-7218.

ORCID

Nav Nidhi Rajput: 0000-0003-4740-8217
Vijayakumar Murugesan: 0000-0001-6149-1702
Larry A. Curtiss: 0000-0001-8855-8006
Karl T. Mueller: 0000-0001-9609-9516

Notes

The authors declare no competing financial interest.

■ ACKNOWLEDGMENTS

This research was intellectually led by the Joint Center for Energy Storage Research (JCESR), an Energy Innovation Hub funded by the U.S. Department of Energy (DOE), Office of Science, Basic Energy Sciences (BES), under Contract No. DEAC02-06CH11357. The calculations were performed using the computational resources of the National Energy Research Scientific Computing Center (NERSC), which is supported by the Office of Science of the U.S. Department of Energy under Contract No. DE-AC02-05CH11231. The NMR measurements were performed at the Environmental Molecular Sciences Laboratory (EMSL), a national scientific user facility sponsored by the DOE's Office of Biological and Environmental Research and located at Pacific Northwest National Laboratory (PNNL). K. C. Lau acknowledges the grants of computer time through the LCRC Blues Cluster and ALCF Vesta Cluster at Argonne National Laboratory.

■ REFERENCES

(1) Scheers, J.; Fantini, S.; Johansson, P. A review of electrolytes for lithium−sulphur batteries. *J. Power Sources* **2014**, *255*, 204−218.
(2) Zhang, S. S. Liquid electrolyte lithium/sulfur battery: fundamental chemistry, problems, and solutions. *J. Power Sources* **2013**, *231*, 153−162.
(3) Bruce, P. G.; Freunberger, S. A.; Hardwick, L. J.; Tarascon, J.-M. Li-O2 and Li-S batteries with high energy storage. *Nat. Mater.* **2012**, *11*, 19−29.
(4) Manthiram, A.; Fu, Y.; Su, Y.-S. Challenges and prospects of lithium−sulfur batteries. *Acc. Chem. Res.* **2012**, *46*, 1125−1134.
(5) Chen, J.; Han, K. S.; Henderson, W. A.; Lau, K. C.; Vijayakumar, M.; Dzwiniel, T.; Pan, H.; Curtiss, L. A.; Xiao, J.; Mueller, K. T.; Shao, Y.; Liu, J. Restricting the Solubility of Polysulfides in Li-S Batteries Via Electrolyte Salt Selection. *Adv. Energy Mater.* **2016**, *6*, 1600160.
(6) Shin, E. S.; Kim, K.; Oh, S. H.; Cho, W. I. Polysulfide dissolution control: the common ion effect. *Chem. Commun.* **2013**, *49*, 2004−2006.

DOI: 10.1021/acs.chemmater.7b00068
Chem. Mater. 2017, 29, 3375−3379

(7) Wujcik, K. H.; Pascal, T. A.; Pemmaraju, C.; Devaux, D.; Stolte, W. C.; Balsara, N. P.; Prendergast, D. Characterization of Polysulfide Radicals Present in an Ether-Based Electrolyte of a Lithium−Sulfur Battery During Initial Discharge Using In Situ X-Ray Absorption Spectroscopy Experiments and First-Principles Calculations. *Adv. Energy Mater.* **2015**, *5*, 1500285.
(8) Partovi-Azar, P.; Kühne, T. D.; Kaghazchi, P. Evidence for the existence of Li 2 S 2 clusters in lithium−sulfur batteries: ab initio Raman spectroscopy simulation. *Phys. Chem. Chem. Phys.* **2015**, *17*, 22009−22014.
(9) Kamphaus, E. P.; Balbuena, P. B. Long-Chain Polysulfide Retention at the Cathode of Li−S Batteries. *J. Phys. Chem. C* **2016**, *120*, 4296−4305.
(10) Assary, R. S.; Curtiss, L. A.; Moore, J. S. Toward a molecular understanding of energetics in Li−S batteries using nonaqueous electrolytes: a high-level quantum chemical study. *J. Phys. Chem. C* **2014**, *118*, 11545−11558.
(11) Vijayakumar, M.; Govind, N.; Walter, E.; Burton, S. D.; Shukla, A.; Devaraj, A.; Xiao, J.; Liu, J.; Wang, C.; Karim, A.; Thevuthasan, S. Molecular structure and stability of dissolved lithium polysulfide species. *Phys. Chem. Chem. Phys.* **2014**, *16*, 10923−10932.
(12) Pascal, T. A.; Pemmaraju, C.; Prendergast, D. X-ray spectroscopy as a probe for lithium polysulfide radicals. *Phys. Chem. Chem. Phys.* **2015**, *17*, 7743−7753.
(13) Wang, L.; Zhang, T.; Yang, S.; Cheng, F.; Liang, J.; Chen, J. A quantum-chemical study on the discharge reaction mechanism of lithium-sulfur batteries. *J. Energy Chem.* **2013**, *22*, 72−77.
(14) Hagen, M.; Schiffels, P.; Hammer, M.; Dörfler, S.; Tübke, J.; Hoffmann, M.; Althues, H.; Kaskel, S. In-situ Raman investigation of polysulfide formation in Li-S cells. *J. Electrochem. Soc.* **2013**, *160*, A1205−A1214.
(15) Pascal, T. A.; Wujcik, K. H.; Velasco-Velez, J.; Wu, C.; Teran, A. A.; Kapilashrami, M.; Cabana, J.; Guo, J.; Salmeron, M.; Balsara, N.; Prendergast, D. X-ray absorption spectra of dissolved polysulfides in lithium−sulfur batteries from first-principles. *J. Phys. Chem. Lett.* **2014**, *5*, 1547−1551.
(16) Pan, H.; Wei, X.; Henderson, W. A.; Shao, Y.; Chen, J.; Bhattacharya, P.; Xiao, J.; Liu, J. On the Way Toward Understanding Solution Chemistry of Lithium Polysulfides for High Energy Li−S Redox Flow Batteries. *Adv. Energy Mater.* **2015**, *5*, 1500113.
(17) Li, Z.; Borodin, O.; Smith, G. D.; Bedrov, D. Effect of Organic Solvents on Li+ Ion Solvation and Transport in Ionic Liquid Electrolytes: A Molecular Dynamics Simulation Study. *J. Phys. Chem. B* **2015**, *119*, 3085−3096.
(18) Shao, Y.; Rajput, N. N.; Hu, J.; Hu, M.; Liu, T.; Wei, Z.; Gu, M.; Deng, X.; Xu, S.; Han, K. S. Nanocomposite polymer electrolyte for rechargeable magnesium batteries. *Nano Energy* **2014**, *12*, 750−759.
(19) Han, K. S.; Rajput, N. N.; Wei, X.; Wang, W.; Hu, J. Z.; Persson, K. A.; Mueller, K. T. Diffusional motion of redox centers in carbonate electrolytes. *J. Chem. Phys.* **2014**, *141*, 104509.
(20) Cheng, L.; Curtiss, L. A.; Zavadil, K. R.; Gewirth, A. A.; Shao, Y.; Gallagher, K. G. Sparingly Solvating Electrolytes for High Energy Density Lithium−Sulfur Batteries. *ACS Energy Lett.* **2016**, *1*, 503−509.

DOI: 10.1021/acs.chemmater.7b00068
Chem. Mater. 2017, 29, 3375−3379